Digital Demodulator for BFSK Waveform Based Upon Correlator and Differentiator Systems

Jorge TORRES[1], Fidel HERNANDEZ[2], Joachim HABERMANN[3]

[1]Dept. of Telecommunication and Telematic, CUJAE University, 114 Street, 11901, La Habana, Cuba
[2]Dept. of Telecommunication and Electronics, UPR University, Marti 270, Pinar del Río, Cuba
[3]Department for ICT, Electrical Engineering & Mechatronics, TH Mittelhessen University of Applied Sciences,D-61169 Friedberg, Germany

[1] jorge.tg@electrica.cujae.edu.cu, [2] fidel@tele.upr.edu.cu, [3] joachim.habermann@iem.thm.de

Abstract. *The present article relates in general to digital demodulation of Binary Frequency Shift Keying (BFSK waveform) . New processing methods for demodulating the BFSK-signals are proposed here. Based on Sampler Correlator, the hardware consumption for the proposed techniques is reduced in comparison with other reported. Theoretical details concerning limits of applicability are also given by closed-form expressions. Simulation experiments are illustrated to validate the overall performance.*

Keywords

BFSK, correlator, digital receiver.

1. Introduction

Frequency Shift Keying (FSK) is a digital modulation with applications in wireless technologies [1] and also in satellite communications [2]. Various configurations of circuitry have previously been reported for BFSK demodulators. As a case in point, there are systems with the Envelope Detector [3] and self-tuning systems [4].

Some of them, specially those based upon correlator receiver employment, are particularly interesting because they perform signal to noise ratio maximization [5] and do not use symbol synchronization blocks. As a case in point, such detectors are Quadricorrelator [6], [7], Balanced Quadricorrelator [7], [8], [9], [10], [11], [12] and Quotient Detector [13].

These types of detectors are implemented in a two-part structure; the first one is an analogue correlator [14]. In the second part, the instantaneous frequency is extracted by performing proper derivation, addition and multiplication procedures, Fig. 1 depicts the case of the Balanced Quadricorrelator. However, due to the large number of adders and multipliers needed, such digital implementations demand a high cost. For instance, the number of floating adders and

multipliers exceeds 47 in the case of the Balanced Quadricorrelator. In this case an elliptic filter is employed for the digital lowpass filter, and a FIR filter of fifth order as a discrete time differentiator [15], both of them employed by the detectors mentioned above.
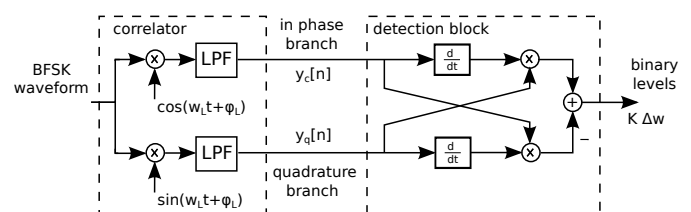

Fig. 1. Block scheme of the balanced quadricorrelator.

Although the low pass filter and the multiplication procedure could be obtained through a flip-flop element, as in the digital logic quadricorrelator scheme [16], and the differentiator can be accomplished by flip-flop blocks followed by AND-gates, this scheme is prone to instabilities under conditions of low signal to noise ratio, causing total interruption of the counting process at the system output, despite of its low hardware consumption.

The method discussed in this paper outperforms all previous schemes, based upon correlator, in a hardware consumption sense. New BFSK detection schemes based upon correlator are devised, which consider the recognition of slope instead of instantaneous frequency at the output of correlator. In this paper, new slope detection algorithm are derived.

2. Receiver Conception

2.1 Correlator Block

The main idea of the proposed receiver is to identify the approximately linear ramp observed at the output of a correlator for a sine-wave input [5]. The BFSK waveform is conformed with only two symbols, comprised by a radio-

frequency pulse with two different frequencies, and they are orthogonal to each other, so if a tone is correlated with itself a linear increase in time is obtained at the output. Conversely, if such a tone is correlated with the other one, approximately a constant output is derived. Figure 2 b) shows the correlation operation for the BFSK signal shown in Fig. 2 a) when the reference is the lower frequency tone.

This behavior is obtained at the output of the correlator when the frequency w_L is the same as the received frequency w_0. Thus, techniques for recovering the average slope leads to new schemes for BFSK demodulators in the detection block. For instance, Fig. 2 c) shows high and low levels in accordance with the signal received in a) when substraction between consecutive points in b) is performed. This aspect will be considered in the next Section in detail.
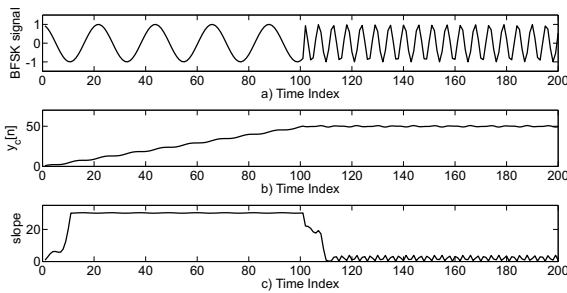

Fig. 2. Output of a correlator for a BFSK-wave input and a sine-wave reference.

In order to reduce complexity a Sampler Correlator [17] is employed instead of other types reported in scientific papers. It is preferred here since it has the same Signal to Noise Ratio (SNR) as the Analogue Correlator [18], which has higher SNR than other types such as the Digital [19], [20] and the Stieltjets [21], [14] receiver. Besides, modified versions of Stieljets [21] or Relay Correlator [19], [22], [23] are implemented with additional sources of random waves which add complexity to the receiver.

Figure 3 depicts the block diagram of the discrete correlator. It is comprised of an IIR filter acting as an accumulator. Besides, the analytic expressions for the output of the in phase branch are described in (1) when a symbol of the type $A\cos(w_i n + \varphi_i)$ is received. At the in-phase branch, in Fig. 3, the summation of $A\cos(w_i n + \varphi_i) \cdot \cos(w_L n + \varphi_L)$ from 0 to n is carried out using the well-known trigonometric identity called Euler's theorem and the sum formula for the geometric progression.
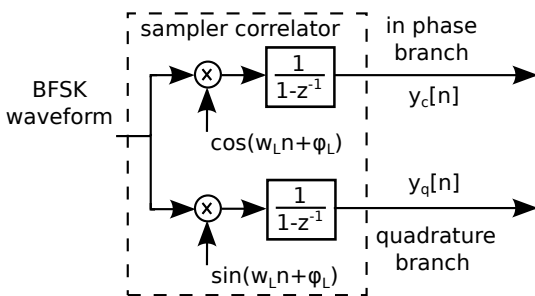

Fig. 3. Sampler correlator scheme.

$$y_c[n] = \frac{A}{4}\left\{ \frac{1}{\sin\left(\frac{w_i - w_L}{2}\right)}\left[\sin\left(\varphi_L - \varphi_i + \frac{w_i - w_L}{2}\right) + \right.\right. \quad (1)$$
$$\left. + \sin\left(\varphi_i - \varphi_L + (w_i - w_L)\left(n + \frac{1}{2}\right)\right)\right] +$$
$$+ \frac{1}{\sin\left(\frac{w_i + w_L}{2}\right)}\left[\sin\left(\frac{w_i + w_L}{2} - \varphi_L - \varphi_i\right)\right.$$
$$\left.\left. + \sin\left(\varphi_i + \varphi_L + (w_i + w_L)\left(n + \frac{1}{2}\right)\right)\right]\right\}.$$

On the other hand, expression (2) describes the case of a received symbol with frequency and phase (w_0, φ_0) and considering also that $w_L = w_0$. This is the case depicted in Fig. 2 b) when the symbol with the lower frequency is being transmitted, where the term $(n + 1)\cos(\varphi_0 - \varphi_1)$ is related to the ramp behavior. The expression (1) also describes the output of the correlator when the high frequency $w_i = w_1$ is received and $w_L = w_0$. The description for the quadrature branch is simply obtained by substituting φ_L by $\varphi_L - \frac{\pi}{2}$ in both expressions (1) and (2)

$$y_c[n] = \frac{A}{2}\left((n+1)\cos(\varphi_0 - \varphi_L) + \right. \quad (2)$$
$$+ \frac{1}{2\sin(w_0)}\left(\sin(w_0 - \varphi_0 - \varphi_L) + \right.$$
$$\left.\left. + \sin\left(2w_0\left(n + \frac{1}{2}\right)\varphi_0 + \varphi_L\right)\right)\right).$$

2.2 Detection Block

Towards detecting the average slope in Fig. 2 the use of a differentiator systems is considered. This is a point of view different to that of the Balanced Quadricorrelator and the others scheme mentioned above. In case of the Balanced Quadricorrelator, the output is directly related to $\Delta w = w_i - w_L$. In the algorithm proposed in this paper, instead of extracting the instantaneous frequency we consider the methods of slope recognition at the correlator output. This is a problem that is also considered in applications for QRS detection [24].

Differentiator systems reported in scientific papers are either based on a FIR discrete-time differentiator [15], or simply perform substraction of consecutive points in the temporal input series. The FIR discrete-time differentiator is equivalent to the ideal derivator $H_d(e^{jw}) = jw\,e^{-jw\frac{M}{2}}$ in the frequency domain, except by additional windowing with Kaiser's window. M represents the filter order and for $M = 5$ a small amplitude approximation error is reported [15].

The differentiator systems without floating multiplier are also described by $H_1(z) = 1 - z^{-1}$, $H_2(z) = 1 - z^{-2}$, $H_4(z) = 2 + z^{-1} - z^{-3} - 2z^{-4}$ or $H_4(z) = 1 - z^{-4}$, first order [25], second order [26], and fourth order [27] respectively. However, a more general case can be considered when the substraction is performed between points at the distance of L samples; in this case, $H_L(z) = 1 - z^{-L}$. Performance analyzes and selection criteria regarding this system are discussed in the Result Section.

The differentiator systems, described above, extract correctly the term $cos(\varphi_0 - \varphi_1)$ from (2), identifying with a high level the interval in wich the symbol of low frequency is received, as in Fig. 2 c). By the other hand, the quadrature branch will detect the term $sin(\varphi_0 - \varphi_1)$ in (2) when φ_L is replaced by $\varphi_L - \frac{\pi}{2}$. After this, the squaring and adding of both branches will neglect the effects of phase in detection.

Figure 4 depicts the general scheme of the receiver with replications of the structure shown in Fig. 3 with different values of w_L; the upper pair of branches are configured for detecting the low frequency, the lower one are configured for the high frequency. The squaring procedures are needed for recovering the energy in both the in phase and quadrature branches. Nevertheless, spurious frequencies must be suppressed in order to obtain the average slope at the output. This can be accomplished through lowpass filters.
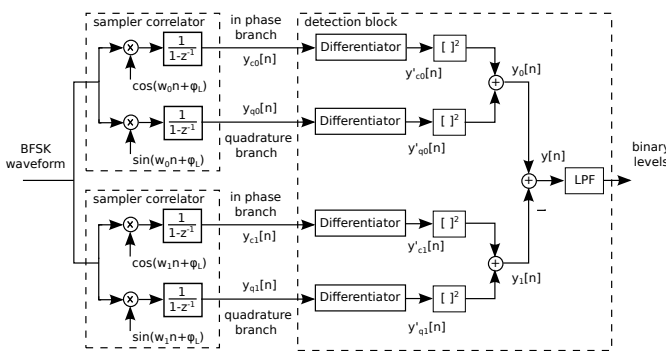

Fig. 4. Block diagram of the receiver.

The differentiator block in Fig. 4 is implemented by means of the transfer function $H_1(z)$, $H_2(z)$, $H_3(z)$ or $H_4(z)$ described above. However, the response function for $H_L(e^{jw}) = -2j \sin(w \frac{L}{2}) e^{jw\frac{L}{2}}$ can also be employed to suppress the high frequencies at the accumulator output. Indeed, the term $\sin(w \frac{L}{2})$ has nulls in the frequency domain when $w \frac{L}{2} = k\pi$, $k \in N$, thus L is a parameter for selecting the null position at frequency w_i by the expression $L = \left\lfloor \frac{2k\pi}{w_i} \right\rfloor$.

In this case the implementation of only one branch, the upper or the lower in Fig. 4, is only needed if a proper expression for the threshold is obtained. Indeed, considering the upper branch for detecting the low frequency, the threshold in (3) is obtained for identifying the high and low levels at $y_0[n]$ in Fig. 4. For further details see the derivation in the Appendix. However, a loss of performance, regarding the

noise margin, is also obtained

$$y_{th} = \frac{1}{2}\left(\frac{A^2}{4}L^2 - |R_{00}| + |R_{01}|\right). \qquad (3)$$

In (3) the term $\frac{A^2}{4}L^2$ is related with the average slope when the symbol of low frequency is detected, R_{00} is related with the amplitude of oscillations around this average slope, and R_{01} represents an upper bound for the oscillations when the symbol of high frequency is received. By way of example, Fig. 5 depicts this values when a BFSK waveform is received with the parameters $w_0 = 0.2856$ rad/s, $w_1 = 0.6347$ rad/s, $f_m = 44100$ Hz, $T_s f_m = 882$ samples, and $L = \left\lfloor \frac{2\pi}{w_0} \right\rfloor = 21$ samples. The value for L was chosen in order to attenuate the term R_{00} in (16) on the Appendix, since it yields the largest oscillation regarding R_{01}. The threshold in (3) is selected as the average between the lines conformed by $\frac{A^2}{4}L^2 - |R_{00}|$ and $|R_{01}|$.
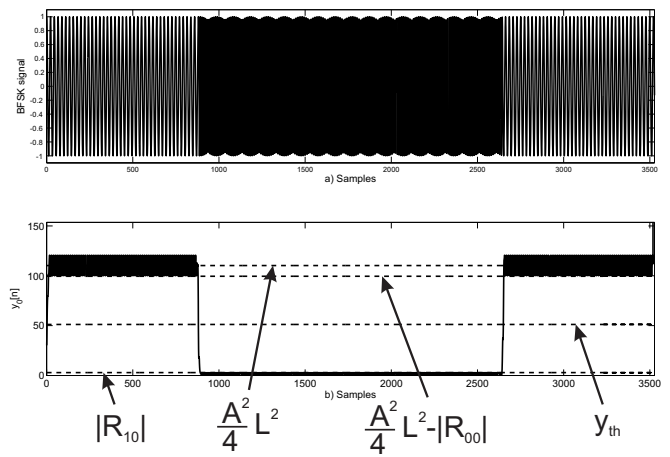

Fig. 5. Performance for the receiver in Figure 4 by means of the $H_L(z)$ differentiator and without the use of a lowpass filter at the output.

2.3 Data Recovery

The recovery of the binary levels from a BFSK waveform using the scheme in Fig. 4 has been described. In this Section the discussion about the performance of digital information associated with the binary data is presented.

After the high and low levels are recovered, as indicated in Figure 6, it is needed to obtain the quantity of "1's" and "0's" that are represented under each level. The length in time of a "1" or a "0" is given by the time-symbol T_s, the comparison of the length of the level and T_s will introduce the quantity of "1's" and "0's" that represents each one. However, this comparison produces errors since the transition of each levels are not abrupt, in this case there is an upper bound on the total of bit to be analyzed. The present section analyzes this situation bringing a closed form expression for determining the quality of the reception.

The algorithm for recovery the data is as follows:

1. Sketching a histogram where the abscissa represents the length of transition in samples; the amplitude is given by the number of occurrences of these lengths. An example is given in Figure 6 b), the abscissa represents the duration of the interval in a). This histogram is used for the estimation of the time-symbol duration.

2. The histogram is comprised of maximal separated by the same distance because the information transmitted consists of successive "1's" or "0's"; thus, in Figure 6 c), the number of samples of each level at the output are multiples of each other. The maximum closer to zero is related to the time-symbol duration, leading to the T_s estimation. The estimation of T_s is obtained with (4), in which N_1 and N_2 represents the interval of the x-axis (e.g. $N_1 = 200$ and $N_2 = 250$ in Figure 6 c), where the histogram has values unequal to zero), T_m represents the sample time, and $h[k]$ represents the values of the histogram obtained

$$\widehat{T_s} = \frac{\sum_{k=N_1}^{N_2} k\, T_m \cdot h[k]}{\sum_{k=N_1}^{N_2} h[k]}. \qquad (4)$$

The length of the high levels in Fig. 6 are established by the intersection of the output of the system with the threshold indicated in (3). In this case, the length of this measure is modified from symbol to symbol by the smooth transition between levels. The accuracy in the determination of T_s, denoted by Δt, could be estimated by calculating the deviation as indicated in Fig. 6 c). The parameters T_s and Δt are related to the binary levels just as indicated in Figure 6 a)

$$\widehat{\Delta t} = \frac{\sum_{k=N_1}^{N_2} (k\, Tm - \widehat{T_s})^2 \cdot h[k]}{\sum_{k=N_1}^{N_2} h[k]}. \qquad (5)$$

3. Once $\widehat{T_s}$ is obtained, the transmitted digital information is recovered by dividing the length of each level with the time-symbol parameter, rounding the result towards the nearest integer.

The accuracy to be obtained on the third step depends on the variance Δt. If k identical symbols are supposed to be transmitted sequentially, then, after many symbols the output in Fig. 4 will have an average duration between symbols of $k \cdot T_s$ plus the variance Δt. If this resulting duration is divided by T_s plus the same Δt, then the total bits to be recovered can be described by the expression (6). Using Laurent expansion and considering $\Delta t << T_s$, we obtain:

$$\widehat{k} = \frac{k \cdot T_s + \Delta t}{T_s + \Delta t} \approx k + (k+1)\frac{\Delta t}{T_s}. \qquad (6)$$
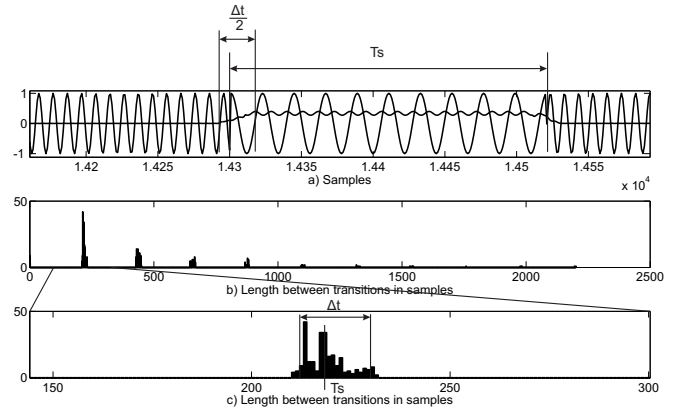

Fig. 6. Details regarding the transition between consecutive symbols. a) Signal received and binary levels. b) Histogram of the length of transitions. c) Horizontal zoom of b).

Expression (6) considers the addition of the variance instead of substraction because the linear system presented in Fig.4 tends to expand the transitions and not to contract. Besides, the same variance is also considered on each transition as a simplification in the determination of accuracy. This considers that the system responds in the same way no matter the total symbols received.

An error in the estimation of k occurs when the second term in (6) is higher than 0.5. In such a case, the estimated value will be superior to $\hat{k} = k + 1$ and the correct value is k. Hence, in the absence of noise the occurrence of consecutive symbols is limited in order to perform a reception free of error.

Equation (7) represents the upper bound for k when T_s and Δt are substituted by $\widehat{T_s}$ and $\widehat{\Delta t}$ respectively, since both of them are obtained via the histogram. Expression (7) gives an idea about how many bits the system in Fig. 2 might receive free of errors in the absence of noise. Indeed, the probability of transmitting k bits comprised of repetitive sequences of "1's" or "0's" is $\frac{1}{2^k}$, so an error could happen once in 2^{k-1} transmitted bits. This is why the receiver is upper bounded in the total of bits to be processed. The relation (7) is a closed form expression that represents a figure of merit for the receivers analyzed, and its values are analyzed in Sec. 3.2

$$k < 0.5 \frac{\widehat{T_s}}{\widehat{\Delta t}} - 1. \qquad (7)$$

3. Results

Three key aspects are considered for comparing the proposed solution with the systems reported:

1. Hardware Complexity

2. Precision through relation (7).

3. Bit Error Rate (BER) performance.

The Balanced Quadricorrelator is less expensive than the Quadricorrelator and the Quotient Detector, and mainly has the best accuracy. Thus, comparison of the system in Figure 4 will be made with regard to the Balanced Quadricorrelator.

3.1 Hardware Complexity

In this Section the complexity is measured with regard to the total of floating adders and multipliers. The total of adders and multipliers to implement the system proposed in Fig. 4 depends upon the employed differentiator. The lowest complexity is obtained when the transfer functions $H_1(z)$, $H_2(z)$, $H_L(z)$ or $H_4(z) = 1 - z^{-4}$, all these systems employ just 1 floating adder. Taking into account one branch in Fig. 4 the total of adders and multipliers is 9, and in cases that 17 is not fulfilled an additional digital filter is also needed.

On the other hand, the Balanced Quadricorrelator employs 2 digital filters, two discrete-time differentiators and 5 additional floating elements for adding and multiplying. The differentiator can be implemented with a FIR of fifth order [15], which requires another 5 adders and 6 multipliers. Summarizing, the total of floating elements is 27 and also 2 digital filters.

In contrast with the Balanced Quadricorrelator, the proposed scheme reduces complexity to 18 floating elements and 1 digital filter. However, in case that the proposed system in Figure 4 is employed with the differentiator $H_L(z)$, without the use of the low pass filter and with only one branch, then in total 7 adders and multipliers are only needed. Which represents a considerable reduction in hardware consumption. This scheme can be employed if relation (17) is fulfilled, this means that oscillations of low levels are not higher than the oscillations of high levels of the binary signal at the output. Besides, relation (18) in the Appendix establishes an upper bound for the total bits to be demodulated by the system, without additional bits and without the presence of noise.

3.2 Precision

Regarding precision, obtained by means of (7), the quantity depends on the parameters of the modulation format. The BFSK waveform is driven by three parameters, f_0, f_1 and T_s, which are related between each other by $f_1 = f_0 + \frac{m}{T_s}$. The simulation is made by holding $f_0 = 1000$ Hz and varying T_s and m as indicated in (8). The parameter r in (8) controls the symbol duration, while m the distance between frequencies

$$f_0 = 1000$$
$$T_s = \frac{r}{f0} \qquad (8)$$
$$f_1 = f_0 + \frac{m}{T_s} = f_0 \left(1 + \frac{m}{r}\right).$$

A family of curves for the k parameter can be obtained when r is the independent variable and m is evaluated for several values. The simulations show that precision is not to much affected with changes in m but with changes in r, these curves are almost the same when $m \geq 4$. Figure 7 shows in average the results for both systems, the Balanced Quadricorrelator and the proposed scheme with one branch and the differentiator $H_L(z)$. The graphic is conformed by averaging the different values given by the variation of m when r is fixed, m is considered in the interval 2 to 20.
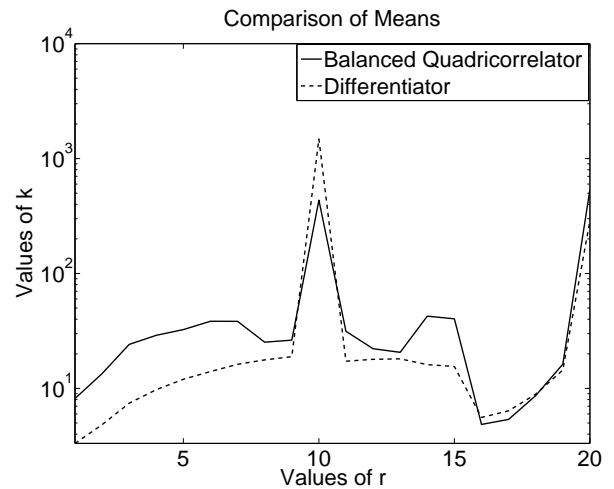

Fig. 7. Precision for different values of r when the different values given by the variation of m when r is fixed, m is considered in the interval 2 to 20.

The curves depicted in Fig. 7 show that the Balanced Quadricorrelator is superior for almost every value of r. This can be explained by the fact the Quadricorrelator performs the operations locally, mainly with the use of discrete-time differentiators, while the proposed scheme estimates slope with samples separated by L points, which further smooth the transitions between levels making it more inaccurate.

3.3 BER Parameter

Figure 7 depicts the measured bit error rate (BER) of the proposed receiver with and without the use of a lowpass filter as a function of the bit energy to power density (SNR), in comparison with that of the Balanced Quadricorrelator. The parameters employed are $w_0 = 0.2856$ rad/s, $w_1 = 0.6347$ rad/s, $f_m = 44100$ Hz, $T_s \cdot f_m = 882$ samples, and $L = \left\lfloor \frac{2\pi}{w_0} \right\rfloor =$

21 samples, the simulation was performed with a total number of 10^6 bits in steps of 0.25 dB on the SNR axis. The range analyzed is below an $\frac{E_b}{N_0}$ of 5 dB since up to this value error correcting codes are usually employed [28].

The proposed receiver without LPF has the worst performance regarding the P_b parameter, and the best performance when the LPF is employed. The lowpass filter reduces the amount of noise in the binary levels, and the Balanced Quadricorrelator in Figure 1 implements both of them on each branch. In contrast, the proposed receiver with the use of only one LPF, saves approximately 1.5 dB of energy regarding the Balanced Quadricorrelator. In both cases, the proposed receiver is used with just one branch.
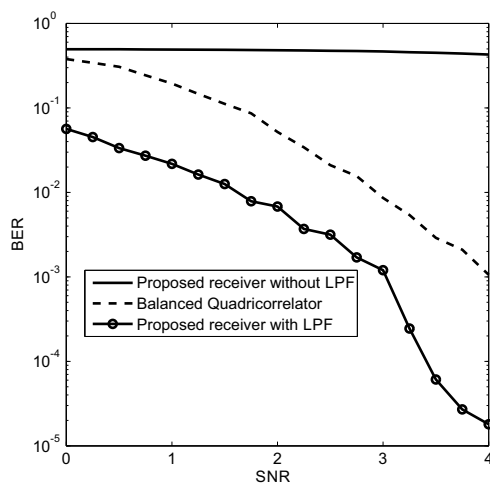

Fig. 8. Bit Error Rate.

At first glance, some of the curves in Fig. 8 suggest a better performance with regard to the ideal receiver. However, the use of lowpass filters in the structures of Fig.1 and Fig. 4 reduces the noise density for the decision rule and this is not the case for the ideal receiver [5].

4. Conclusions

The solution presented proposes a different detection scheme for the Balanced Quadricorrelator regarding to the detection scheme. High-order filters are avoided thanks to one important matter: the symbol detection is accomplished through the constant slope recognition verified at the output of Sampler Correlator. Although this simple scheme exhibits fluctuations at the output that restrict proper symbol identification, this could be avoided by means of a lowpass filter. However, the entire solution has less complexity than other reported methods. The proposed solution based upon correlator maximizes signal to noise ratio at the input detector like previous solutions, but with a major advantage: it reduces complexity for hardware implementation. Accordingly, advantages of lower energy consumption and hardware saving are also provided.

Appendix

In the present Section it is derived a closed-form expression for the output of system in Fig. 4, when a differentiator with transfer function $H_L(z) = 1 - z^{-L}$ is considered. Consider that a symbol $A\cos(w_0 n + \varphi_0)$ is received; the expression (9), corresponding to the output of the differentiator of the in phase branch that detects the frequency w_1, Fig. 4, is obtained by grouping terms with the trignometric relations in (10). The upper bound for (9) is obtained in (11) taking into account (12). The upper bound for the quadrature branch $y'_{s1}[n]$ is the same, since the phase is not present in the expression for the upper bound

$$
\begin{aligned}
y'_{c1}[n] =& y_{c1}[n] - y_{c1}[n-L] \qquad\qquad (9)\\
=& a\cos\left(\varphi_0 - \varphi_L + (w_0 - w_1)\left(n - \frac{L}{2} + \frac{1}{2}\right)\right) + \\
&+ b\cos\left(\varphi_0 + \varphi_L + (w_0 + w_1)\left(n - \frac{L}{2} + \frac{1}{2}\right)\right)
\end{aligned}
$$

$$
a = \frac{A}{2}\,\frac{\sin\left(\frac{L(w_0 - w_L)}{2}\right)}{\sin\left(\frac{w_0 - w_L}{2}\right)}
$$

$$
b = \frac{A}{2}\,\frac{\sin\left(\frac{L(w_0 + w_1)}{2}\right)}{\sin\left(\frac{w_0 + w_1}{2}\right)},
$$

$$
\cos(A) - \cos(B) = 2\sin\left(\frac{B+A}{2}\right)\sin\left(\frac{B-A}{2}\right) \qquad (10)
$$

$$
\sin(A) - \sin(B) = 2\cos\left(\frac{B+A}{2}\right)\sin\left(\frac{A-B}{2}\right),
$$

$$
|y'_{c1}[n]| \le \frac{A}{2}\left|\frac{\sin\left(\frac{L(w_0 - w_1)}{2}\right)}{\sin\left(\frac{w_0 - w_1}{2}\right)}\right| + \frac{A}{2}\left|\frac{\sin\left(\frac{L(w_0 + w_1)}{2}\right)}{\sin\left(\frac{w_0 + w_1}{2}\right)}\right|, \quad (11)
$$

$$
A\cos(\theta + \alpha) + B\cos(\theta + \beta) \le C \qquad\qquad (12)
$$

$$
C = \sqrt{A^2 + B^2 + 2AB\cos(\alpha - \beta)}
$$

$$
A\cos(\theta + \alpha) + B\cos(\theta + \beta) \le |A| + |B|.
$$

Since $y'_{c1}[n]$ is in quadrature respect to $y'_{q1}[n]$, the upper bound for $y'_{c1}[n]^2 + y'_{q1}[n]^2$ is just the square of the upper bound of $y'_{c1}[n]^2$ or $y'_{q1}[n]^2$. Thus, a symbol with frequency w_0 produces, at the output of the branch, an upper bound determined by relation (14)

$$|y_1[n]| \le R_{01} \tag{13}$$

$$R_{01} = \frac{A^2}{4} \left[\left| \frac{\sin\left(\frac{L(w_0 - w_1)}{2}\right)}{\sin\left(\frac{w_0 - w_1}{2}\right)} \right| + \left| \frac{\sin\left(\frac{L(w_0 + w_1)}{2}\right)}{\sin\left(\frac{w_0 + w_1}{2}\right)} \right| \right]^2.$$

The case for the branch that detects w_0 is shown in (14). Through the operation $y'_{c0}[n] = \lim_{w_1 \to w_0} y'_{c1}[n]$, the term $\cos(\varphi_0 - \varphi_L)\frac{A}{2}L$ is related to the constant behavior in Figure 2 c)

$$y'_{c0}[n] = \cos(\varphi_0 - \varphi_L)\frac{A}{2}L + R_{c0} \tag{14}$$

$$R_{c0} = \frac{A}{2}\frac{\sin(w_0 L)}{\sin(w_0)}\cos\left(\varphi_0 + \varphi_L + 2w_0\left(n - \frac{L}{2} + \frac{1}{2}\right)\right)$$

$$|R_{c0}[n]| \le \frac{A}{2}\left|\frac{\sin(w_0 L)}{\sin(w_0)}\right|.$$

The differentiator output for the in quadrature branch is obtained in (15) by changing φ_L by $\varphi_L - \pi$ in (14)

$$y'_{s0}[n] = -\sin(\varphi_0 - \varphi_L)\frac{A}{2}L + R_{s0}[n] \tag{15}$$

$$R_{s0}[n] = \frac{A}{2}\frac{\sin(w_0 L)}{\sin(w_0)}\sin\left(\varphi_0 + \varphi_L + 2w_0\left(n - \frac{L}{2} + \frac{1}{2}\right)\right)$$

$$|R_{s0}[n]| \le \frac{A}{2}\left|\frac{\sin(w_0 L)}{\sin(w_0)}\right|.$$

Finally, the output of the branch that detects the frequency w_0 is obtained in (16) by straightforward procedures

$$y_0[n] = y'_{c0}{}^2[n] + y'_{s0}{}^2[n] \tag{16}$$

$$= \frac{A^2}{4}L^2 + R_{00}[n]$$

$$|R_{00}[n]| \le \frac{A^2 L}{2}\left|\frac{\sin(w_0 L)}{\sin(w_0)}\right| + \frac{A^2}{4}\frac{\sin^2(w_0 L)}{\sin^2(w_0)}.$$

A proper detection of the symbol with frequency w_0 is obtained if the condition $y_0[n] > y_1[n]$ is fulfilled during the interval duration of such a symbol. Upon substituting (12) and (16) in the condition above, and considering the worst case, that is a negative value for $R_{00}[n]$, (17) is obtained

$$\frac{A^2}{4}L^2 - |R_{00}| - |R_{01}| > 0. \tag{17}$$

Even further, the L parameter is directly related to the precision of the system. The longer the L value is, the longer will be the transition between symbols in Fig. 6. Thus, in relation (7), the L parameter is directly related to the variance in the determination of the symbol transition Δt and

(18) gives a measure of the total bits, in average, to be analyzed without errors; N_{samp} represents the number of samples per symbol

$$k < 0.5\frac{N_{samp}}{L} - 1. \tag{18}$$

Expressions (18) and (17) give the rules for the proper performance of the system given in Figure 4 with a differentiator $H_L(z) = 1 - z^{-L}$. The latter evaluate L for a given precision, the former determines if a filter at the output is needed.

References

[1] PENG, K.-C., LIN, C.-C., CHAO, C.-H.. A novel three-point modulation technique for fractional-N frequency synthesizer applications, *Radioengineering*. 2013, vol. 22, no. 1, p. 269–275.

[2] VERTAT, I., MRAZ, J. Hybrid M-FSK/DQPSK modulations for CubeSat picosatellites, *Radioengineering*. 2013, vol. 22, nol. 1, p. 389–393.

[3] THOMPSON, A. C., HUSSAIN, Z. M., O'SHEA P. A single-bit digital non-coherent baseband BFSK demodulator, *In IEEE Region 10 Conference TENCON*. 2004, vol. 1, p. 515–518.

[4] TERVO, R., ZHOU, K. DSP based self-tuning BFSK demodulation, *In IEEE Pacific Rim Conference on Communications, Computers and Signal Processing*, 1993, vol. 1, p. 68–71.

[5] SKLAR, B. *Digital Communications, Fundamental and Applications*, 2nd ed. New Jersey: Prentice Hall, 2001.

[6] RICHMAN, D. Color-carrier reference phase synchronization accuracy in NTSC color television. *Proceedings of the IRE*, 1954, vol.42, no.1, p. 106–133.

[7] GARDNER, F., Properties of Frequency Difference Detectors. *In IEEE Transactions on Communications*,1985, vol. 33, no. 2, p. 131–138.

[8] PARK, J., An FM detector for low S/N. *IEEE Transactions on Communication Technology*, 1970, vol. 18, no. 2, p. 110–118.

[9] NATALI, F., AFC tracking algorithms. *IEEE Transactions on Communications*, 1984, vol. 32, no. 8, p. 935–947.

[10] FARRELL, K., A., McLANE, P., J. Performance of the cross-correlator receiver for binary digital frequency modulation. *IEEE Transactions on Communications*, 1997, vol. 45, no. 5, p. 573–582.

[11] KANG, H., KIM, D., PARK, S.C. Coarse frequency offset estimation using a delayed auto-quadricorrelator in OFDM-based WLANs, In *3rd International Congress on Ultra Modern Telecommunications and Control Systems and Workshops (ICUMT)*, 2011, p. 1–4.

[12] ORDU, G., KRUTH, A., SAPPOK, S., WUNDERLICH, R., HEINEN. S. A quadricorrelator demodulator for a Bluetooth low-IF receiver. In *IEEE Radio Frequency Integrated Circuits (RFIC) Symposium. Digest of Papers*. 2004, p. 351–354.

[13] KREUZGRUBER, P. A class of binary FSK direct conversion receivers. In *IEEE 44th Vehicular Technology Conference,* . 1994, vol. 1, p. 457–461.

[14] EGAU, PC. Correlation systems in radio astronomy and related fields.In *IEEE Proceedings F Communications, Radar and Signal Processing*. 1984, vol. 131, no. 1, p. 32–39.

[15] OPPENHEIM, A., V., SCHAFER, R., W., BUCK, J., R. *Discrete-Time Signal Processing*. 2nd ed. New Jersey: Prentice Hall, 1998.

[16] AHN, T., YOON, C.-G., MOON, Y. An adaptive frequency calibration technique for fast locking wideband frequency synthesizers, In *48th Midwest Symposium on Circuits and Systems*. 2005, vol. 2, p. 1899–1902.

[17] LEE, Y., W., CHEATHAM, T., P., WIESNER, J., B. Application of correlation analysis to the detection of periodic signals in noise, *Proceedings of the IRE*, 1950, vol. 38, no. 10, p. 1165–1171.

[18] PEEK, J., B., H. The measurement of correlation functions in correlators using "shift-invariant independent functions", *Philips Res. Rep. Suppl*. 1968, vol. 1.

[19] CHANG, K.-Y., MOORE, A. Modified digital correlator and its estimation errors, *IEEE Transactions on Information Theory*, 1970, vol. 16, no. 6, p. 699–706.

[20] VAN VLECK, J., H. *The spectrum of clipped noise*, Tech. Rep. No. 51. Cambridge, Mass., Radio Res. Lab., Harvard University, 1943.

[21] WATTS, D., G. A general theory of amplitude quantization with applications to correlation determination, *Proceedings of the IEEE - Part C: Monographs*. 1962, vol. 109, no. 15, p. 209–218.

[22] JESPER, P., CHU, P., T., FETTWEIS, A: A new method to compute correlation functions, In *Int. Symp. Inform. Theory, and IRE Trans. Inform. Theory*. 1962, p. 106–107.

[23] BERNDT, H., Correlation function estimation by a polarity method using stochastic reference signals, *IEEETransactions* 1968, IT-14, p.796–801.

[24] ARZENO, N. M., DENG, Z. D., POON C. S. Analysis of first-derivative based QRS detection algorithms, *IEEE Transactions on Biomedical Engineering*. 2008, vol. 55, no. 2, p.478–84.

[25] MUKHOPADHYAY, S., MITRA, M., MITRA, S. Time plane ECG feature extraction using hilbert transform, variable threshold and slope reversal approach, In *2011 International Conference on Communication and Industrial Application (ICCIA)*. 2011, p. 1–4.

[26] FRIESEN, G., JANNET, T., JADALLAH, M., YATES, S., QUINT, S., Nagle, H. A comparison of the noise sensitivity of nine QRS detection algorithms, *IEEE Transactions on Biomedical Engineering*, 1990, vol. 37, no. 1, p. 85–98, 1990.

[27] ARZENO, N., DENG, Z., D., POON, C., S. Analysis of first-derivative based QRS detection algorithms, *IEEE Transactions on Biomedical Engineering*, 2008, vol. 55, no. 2, p. 478–484.

[28] CARLSON, A., B., Crilly, P., B., RUTLEDGE, J., C. Communication systems: an introduction to signals and noise in electrical communication, 4th ed .McGraw-Hill, 2002.

About Authors. . .

Jorge TORRES received his M.Sc. from CUJAE university in 2010. His research interests include digital demodulation, digital signal processing, estimation theory. He is currently a full assistant professor at CUJAE University, Habana, Cuba.

Fidel HERNANDEZ M.Sc. in Digital Systems from CUJAE in 2000, Ph.D. degree in Electronics and Industrial Automation from University of Mondragon, Spain, in 2006. Currently he works as full professor in University of Pinar del Rio, Cuba. Head of the Research Group for Advanced Machine Diagnosis (GIDAM) since 2000. He has directed several international and national projects involving eye image processing for medical diagnostic applications, higher-order statistical signal processing applied on mechanical vibrations, classification and demodulation of communication signals, and so on. He is a CYTED expert, and is associate editor and reviewer of various international journals. He is member of the administration committee of the Cuban Association of Pattern Recognition.

Joachim HABERMANN is currently a full professor in the Department of Electrical Engineering and Information Technology of the Technische Hochschule Mittelhessen (THM), University of Applied Sciences Giessen, Germany. He obtained his Diploma and Dr.-Ing. (Ph.D.) degrees in Electrical Engineering both with highest honors from the Technical University of Darmstadt, Germany. Prior to joining THM he worked in the Asea Brown Boveri (ABB) research center, Switzerland in the Telecommunications department as a researcher and project leader. He was part of the working groups defining the global mobile communication systems GSM and UMTS and is now a contributor to the development of the enhanced LTE system. He has authored and coauthored more than 70 technical papers in journals and international conferences and one textbook. He is a senior member of the Institute of Electrical and Electronics Engineers (SM IEEE) and served as Technical Chair and member of the program committee of many international conferences. He is also reviewer of several research institutions, such as the German Research Council (DFG).